JOURNAL OF GEOPHYSICAL RESEARCH, VOL. 103, NO. C13, PAGES 31,033–31,044, DECEMBER 15, 1998

Variations of light absorption by suspended particles with chlorophyll *a* concentration in oceanic (case 1) waters: Analysis and implications for bio-optical models

Annick Bricaud, André Morel, Marcel Babin, Karima Allali, and Hervé Claustre

Laboratoire de Physique et Chimie Marines, Université Pierre et Marie Curie and CNRS, Villefranche-sur-Mer Cedex, France

Abstract. Spectral absorption coefficients of total particulate matter $a_p(\lambda)$ were determined using the in vitro filter technique. The present analysis deals with a set of 1166 spectra, determined in various oceanic (case 1) waters, with field chl *a* concentrations ($\langle chl \rangle$) spanning 3 orders of magnitude (0.02–25 mg m^{-3}). As previously shown [*Bricaud et al.*, 1995] for the absorption coefficients of living phytoplankton $a_\phi(\lambda)$, the $a_p(\lambda)$ coefficients also increase nonlinearly with $\langle chl \rangle$. The relationships (power laws) that link $a_p(\lambda)$ and $a_\phi(\lambda)$ to $\langle chl \rangle$ show striking similarities. Despite large fluctuations, the relative contribution of nonalgal particles to total absorption oscillates around an average value of 25–30% throughout the $\langle chl \rangle$ range. The spectral dependence of absorption by these nonalgal particles follows an exponential increase toward short wavelengths, with a weakly variable slope (0.011 ± 0.0025 nm^{-1}). The empirical relationships linking $a_p(\lambda)$ to $\langle chl \rangle$ can be used in bio-optical models. This parameterization based on in vitro measurements leads to a good agreement with a former modeling of the diffuse attenuation coefficient based on in situ measurements. This agreement is worth noting as independent methods and data sets are compared. It is stressed that for a given $\langle chl \rangle$, the $a_p(\lambda)$ coefficients show large residual variability around the regression lines (for instance, by a factor of 3 at 440 nm). The consequences of such a variability, when predicting or interpreting the diffuse reflectance of the ocean, are examined, according to whether or not these variations in a_p are associated with concomitant variations in particle scattering. In most situations the deviations in a_p actually are not compensated by those in particle scattering, so that the amplitude of reflectance is affected by these variations.

1. Introduction

Radiative transfer studies have established analytical links between the apparent optical properties (AOP) of the ocean [*Preisendorfer*, 1961] and its inherent optical properties (IOP), namely, the absorption and scattering properties of the water column [e.g., *Gordon et al.*, 1975; *Kirk*, 1981; *Mobley*, 1994]. Therefore, when developing bio-optical models, such as for predicting the propagation of the radiant energy within the ocean or interpreting ocean color observations, there is a need to express the bulk IOPs or the contributions of the various substances to each of these coefficients as functions of their content in seawater. In oceanic "case 1" waters, the substances determining the IOPs, besides water itself, are (1) living phytoplankton; (2) associated "nonalgal" particles, such as biogenous detritus and heterotrophic organisms; and (3) colored dissolved organic matter (CDOM) resulting from biological activity. Therefore analytical bio-optical models should ideally include parameterizations of IOPs for each of these components.

This has generally not been the case because of the variability in the individual spectral signatures of these various components as well as in the natural relationships existing between their concentrations. *Prieur and Sathyendranath* [1981] first proposed a parameterization of the total (particulate + dissolved) absorption coefficient at 440 nm, $a(440)$, that was derived from measurements of the diffuse attenuation coefficient K_d (see notation section). Direct parameterizations of $K_d(\lambda)$, which is related to $a(\lambda)$, have also been proposed for the visible spectrum [*Smith and Baker*, 1978, *Morel*, 1988; *Gordon et al.*, 1988]. These various studies have shown that either a or K_d vary nonlinearly with the chlorophyll *a* concentration in the water body (hereinafter denoted as $\langle chl \rangle$). This nonlinearity was generally ascribed to the increasing proportion of nonalgal particles with decreasing chl *a* concentration. Besides nonalgal particles, a and K_d also include the contribution of CDOM, which has to be taken into account [*Baker and Smith*, 1982]. While this contribution is generally thought to be weak in the open ocean, its importance relative to that of other compartments is poorly known. Finally, the K_d coefficient also depends on scattering, which may contribute to the nonlinear character of the relationship between K_d and $\langle chl \rangle$ [*Kirk*, 1981; *Gordon et al.*, 1988].

A further step in bio-optical models is to consider separately the particulate and dissolved compartments, where the particulate compartment includes both living phytoplankton and nonalgal matter. Direct spectral measurements of particulate absorption $a_p(\lambda)$ using the filter technique [*Trüper and Yentsch*, 1967] have been performed more and more frequently, allowing variations in these coefficients to be studied [*Mitchell and Kiefer*, 1988; *Garver et al.*, 1994; *Cleveland*, 1995]. Such measurements also allow the respective contributions of the living phytoplankton a_ϕ and nonalgal particles a_{nap} (with $a_p = a_\phi + a_{nap}$) to be estimated, using either experimental

Paper number 98JC02712.
0148-0227/98/98JC-02712$09.00

Table 1. Cruises in Which Absorption Data Were Collected

Cruise	Location	Period	Water Type
PACIPROD	Peru upwelling	Aug.–Sept. 1986	M
CHLOMAX	Sargasso Sea	Sept.–Oct. 1987	O
LIDAR 89	St. Lawrence estuary and gulf	Sept. 1989	E, M
LIDAR 90	St. Lawrence estuary and gulf	July 1990	E, M
TOMOFRONT	northwestern Mediterranean	April 1990	M
MEDIPROD 6	southwestern Mediterranean	July 1990	E, M
EUMELI 3	tropical North Atlantic	Oct. 1991	M, O
EUMELI 4	tropical North Atlantic	June 1992	E, M, O
FLUPAC	equatorial and subequatorial Pacific	Sept.–Oct. 1994	O, M
OLIPAC	equatorial and subequatorial Pacific	Nov. 1994	O, M
MINOS	eastern and western Mediterranean	May 1996	O, M

M, O, and E denote mesotrophic, oligotrophic, and eutrophic, respectively.

[e.g., *Kishino et al.*, 1985] or numerical [e.g. *Morrow et al.*, 1989; *Bricaud and Stramski*, 1990] techniques. Systematic studies [*Bricaud et al.*, 1995; *Cleveland*, 1995] have shown that $a_\phi(\lambda)$ varies in a nonlinear manner with ⟨chl⟩, as a result of changes in pigment composition and in the package effect with the trophic state of waters. Furthermore, the exponent in the power law that links a_ϕ to ⟨chl⟩ (e.g., 0.67 at the blue maximum [*Bricaud et al.*, 1995]) is very close to that previously found for K_d (0.71 [*Morel*, 1988]); note that K_d depends on a_p rather than solely on a_ϕ. The similarity of these exponents suggests that the relative contribution of nonalgal particles to absorption does not vary markedly with ⟨chl⟩ and is not the source of the nonlinear variations in total absorption, as previously assumed [e.g., *Gordon et al.*, 1988].

It is therefore timely to examine how the particulate absorption coefficients vary with ⟨chl⟩ and to what extent the nonalgal particulate matter contributes to total particulate absorption. The consistency of the variations in $a_p(\lambda)$ and $K_d(\lambda)$ with ⟨chl⟩ will also be examined. Finally, particular attention will be paid to the natural variability of particulate absorption, with its implications for bio-optical models, particularly those aimed at predicting the diffuse reflectance of the ocean.

2. Data and Methods

The present data set includes 783 samples previously used for studying the variations in phytoplanktonic absorption [*Bricaud et al.*, 1995] and collected during eight cruises in various areas of the world ocean. From the original data set, 32 samples have been removed as containing nonbiological detrital matter, so that only case 1 waters are included in this data set. In addition, the present data set also includes 383 new samples, collected during the following three recent cruises: (1) the FLUPAC cruise in September–October 1994 (Joint Global Ocean Flux Study (JGOFS) France program) [*Le Borgne and Gesbert*, 1995], where measurements were performed in the oligotrophic and mesotrophic waters of the equatorial Pacific, along a meridian transect at 165°E (from 15°S to 6°N) and a transect along the equator between 167°E and 150°W (84 spectra); (2) the OLIPAC cruise in November 1994 (JGOFS France program [*Moutin and Coste* 1996]), also in the equatorial Pacific, along a transect at 150°W between 16°S and 1°N (184 spectra); and (3) the MINOS cruise in May 1996 in waters ranging from ultraoligotrophic waters (eastern Mediterranean Sea) to mesotrophic waters in the Western Basin (115 spectra). Information concerning the various cruises is summarized in Table 1. Only samples collected in the 0 to 200-m layer have been considered in the present data set.

Methods are described in detail by *Bricaud et al.* [1995]. Briefly, particulate absorption coefficients $a_p(\lambda)$ were determined using the glass-fiber filter (GF/F) technique, except for the FLUPAC cruise, where the "glass-slide technique" [*Allali et al.*, 1995] was used. All a_p spectra were set to 0 at 750 nm. Although this may be not strictly true for detrital matter, this assumption is believed to minimize possible differences between sample and reference filters. Then the spectra measured using the GF/F technique were corrected for the path length amplification effect, using the algorithm given by *Bricaud and Stramski* [1990] for the previous data set and that given by *Allali et al.* [1997] for the three additional cruises. This latter algorithm, derived from measurements in the equatorial Pacific and providing slightly lower values than the Bricaud and Stramski algorithm (by 15% for an optical density of 0.3), is thought to be more appropriate for oligotrophic waters (see discussion by *Allali et al.* [1997]). Finally, the contributions of phytoplankton $a_\phi(\lambda)$ and nonalgal matter $a_{\mathrm{nap}}(\lambda)$ to total particulate absorption were determined either experimentally [*Kishino et al.*, 1985] or by numerical decomposition [*Bricaud and Stramski*, 1990; see *Bricaud et al.*, 1995, Table 1]. For the three recent cruises, numerical decomposition was always used (for a few samples the method of Kishino et al. was also applied for verification). It is recalled here that Kishino et al.'s method does not provide $a_\phi(\lambda)$ and $a_{\mathrm{nap}}(\lambda)$ sensu stricto but, rather, the absorption coefficients of pigmented matter (at least that extractable in methanol) and nonpigmented matter.

Pigment concentrations were measured using various techniques (high pressure liquid chromatography (HPLC), spectrofluorometry, fluorometry, spectrophotometry). The HPLC method was considered as the reference, and for the previous data set some corrections were made to account for systematic divergences between HPLC and other methods [see *Bricaud et al.*, 1995]. For the three recent cruises, measurements were always made using the HPLC technique, according to the procedure described by *Vidussi et al.* [1996]. Absorption coefficients (a_p, a_ϕ, a_{nap}) were converted into chl-specific coefficients (a_p^*, a_ϕ^*, a_{nap}^*) by normalizing to the chl *a* concentration (including divinyl-chl *a* and pheophytin *a*, if any).

3. Results and Discussion

3.1. Relationship Between Particulate Absorption (at 440 nm) and Chlorophyll *a* Concentration

The particulate absorption coefficient $a_p(440)$ exhibits a clear trend of increasing nonlinearly with ⟨chl⟩ (see log-log plot in Figure 1a), as observed previously for the phytoplankton

absorption coefficient [*Bricaud et al.*, 1995]. As a first approximation, power functions are appropriate to represent these variations. For the wavelength 440 nm, where $a_p(\lambda)$ and $a_\phi(\lambda)$ are near their maximum (the spectral values will be considered later), least squares fits provide the following relationships:

$$a_p(440) = 0.0520\ \langle \text{chl} \rangle^{0.635}, \qquad r^2 = 0.91,\ N = 1166 \qquad (1)$$

$$a_\phi(440) = 0.0378\ \langle \text{chl} \rangle^{0.627}, \qquad r^2 = 0.90,\ N = 1166 \qquad (2)$$

where r^2 is the determination coefficient and N is the number of samples. Note that (2) slightly differs from the expression previously given by *Bricaud et al.* [1995] as it is derived from a larger data set (1166 versus 815 samples).

The nonlinear character of (1) appears very similar to that previously found by *Morel* [1988] for the nonwater diffuse attenuation coefficient ($K_d - K_w$), hereinafter referred to as K_{bio}:

$$K_{bio}(440) = 0.1041\ \langle \text{chl} \rangle^{0.707}, \qquad r^2 = 0.94$$

although the K_{bio} values are, on average, twice as high as the a_p values, as a consequence of the contribution of absorption by CDOM and of the effect of scattering.

Equations (1) and (2) can be straightforwardly transformed into

$$a_p^*(440) = 0.0520\ \langle \text{chl} \rangle^{-0.365} \qquad (1')$$

$$a_\phi^*(440) = 0.0378\ \langle \text{chl} \rangle^{-0.373} \qquad (2')$$

where the starred quantities represent the chl-specific coefficients ($m^2\ mg^{-1}$). Nonlinear relationships similar to (1′) were previously found by *Yentsch and Phinney* [1989] at 440 nm and by *Garver et al.* [1994] for particulate absorption averaged over the visible spectrum (but only for ⟨chl⟩ values lower than 1 mg m^{-3}).

The exponents in (1) and (2) are remarkably close, and the variations of $a_p(440)$ and $a_\phi(440)$ versus ⟨chl⟩ are nearly parallel (Figure 1), which suggests that at this wavelength, absorption by nonalgal particles is roughly proportional to total absorption. This is also suggested by the relationship directly established between $a_{nap}(440)$ and ⟨chl⟩:

$$a_{nap}(440) = 0.0124\ \langle \text{chl} \rangle^{0.724}, \qquad r^2 = 0.73 \qquad (3)$$

in which the exponent is not appreciably different from those in (1) and (2) (note, however, the much lower determination coefficient for a_{nap}). According to (1) and (2), $a_p(440)$ is higher than $a_\phi(440)$ by, on average, a factor 1.37 over the entire ⟨chl⟩ range (from 1.33 when ⟨chl⟩ = 0.02 mg m^{-3} to 1.41 when ⟨chl⟩ = 25 mg m^{-3}). In other words, living phytoplankton and nonalgal particles would contribute, on average, 73% and 27%, respectively, to total particulate absorption at 440 nm.

It is worth noting that the scatter for a_p (actually high throughout the whole ⟨chl⟩ range) is not larger than that for a_ϕ, as the determination coefficients on the log-transformed data are almost identical (0.90). Residuals are nearly normally distributed around the regression lines, which allows confidence intervals to be computed for delimiting the natural variability in these coefficients. The dashed lines in Figure 1a delimit the prediction intervals at a 90% confidence level and can be considered as realistic upper and lower limits. According to these prediction intervals, the $a_p(440)$ values may vary by a factor of 2.9 for a given ⟨chl⟩ value. Oligotrophic waters

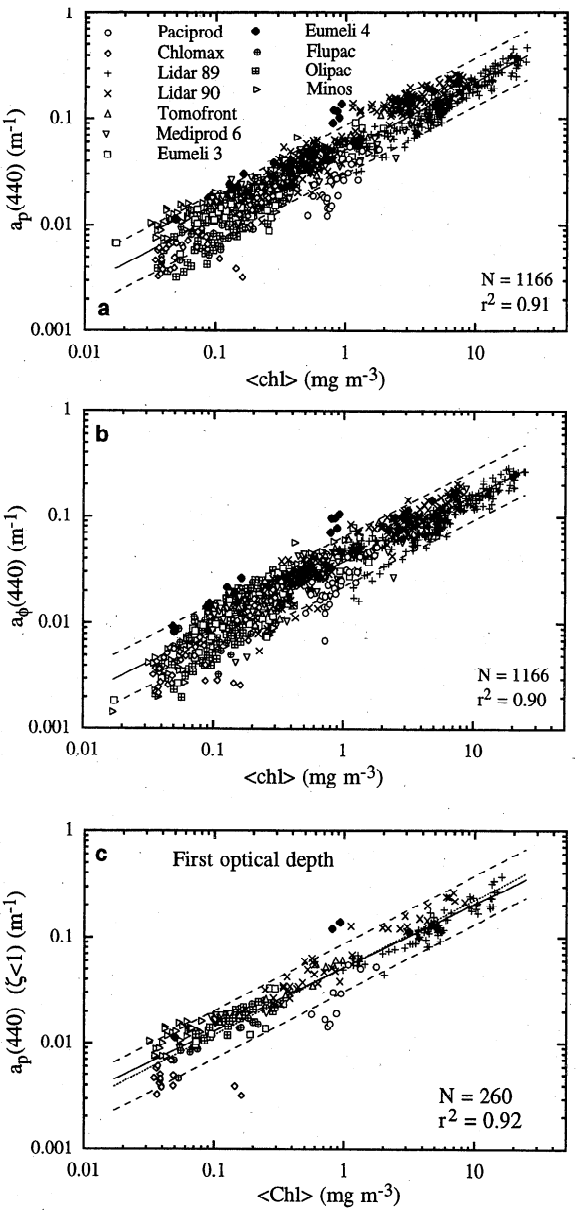

Figure 1. (a) Variations of the absorption coefficients of particles at 440 nm, $a_p(440)$, as a function of ⟨chl⟩, for various regions of the world ocean (see Table 1). All depths have been pooled together. The regression line (equation (1)) is shown as a solid line; the dashed lines delimit the prediction interval at a 90% confidence level. Here ⟨chl⟩ represents the (chl *a* + DV-chl *a* + pheo *a*) concentration. (b) Same as Figure 1a, but for the absorption coefficient of living phytoplankton $a_\phi(440)$. The equation of the regression line is (2). (c) Same as Figure 1a, but for the samples located within the first optical depth ($z = z_e/4.6$, where z_e is euphotic depth). The equation of the regression line is (4) (solid line). The regression line and prediction interval corresponding to the whole data set (as in Figure 1a) are also shown (dotted and dashed lines) for comparison.

(with ⟨chl⟩ <0.1 mg m^{-3}) actually encompass this range, while eutrophic waters span a more restricted range. This might be the result of geographical diversity, which was larger for oligotrophic waters than for eutrophic waters in our data set. For mesotrophic waters, some groups of points stand apart, particularly data from the EUMELI 4 cruise (above the upper limit)

and data from the PACIPROD and CHLOMAX cruises (below the lower limit).

A similar range of variation (a factor of 2.95) is observed for $a_\phi(440)$ (Figure 1b). Groups of points outside these limits are also observed for the EUMELI 4 and CHLOMAX cruises, which means that for these particular samples, anomalously high or low a_p values can be attributed to algae (by virtue, for instance, of a particular pigment composition) and not to nonalgal particles. Samples from the mesotrophic site during the EUMELI 4 cruise were characterized by an exceptionally high concentration of cyanobacteria [*Morel*, 1997] and therefore by a high zeaxanthin content relative to ⟨chl⟩. In contrast, most $a_\phi(440)$ data from the PACIPROD cruise are low but not "anomalous," so that the very low a_p values appear to result from a weak contribution of nonalgal particles to total absorption.

When computing the prediction intervals throughout the visible spectrum (not shown), it is observed that for a given ⟨chl⟩ value, $a_p(\lambda)$ varies by a factor of 2.8 to 4 according to wavelength, except in the green part of the spectrum where it becomes even higher (likely because of the increasing experimental uncertainty affecting a_p in this spectral domain). Such relatively high scatter around the mean $a_p(\lambda)$ versus ⟨chl⟩ relationships may originate from geographical or seasonal differences. From a restricted data set, *Carder et al.* [1991] discerned different tendencies between temperate and subtropical waters. In contrast, *Cleveland* [1995] did not detect distinct patterns for these regions but only for subpolar (Arctic) waters, in agreement with previous findings of *Mitchell and Holm-Hansen* [1991] for Antarctic waters. For the South Atlantic Bight shelf waters, *Nelson and Guarda* [1995] observed season-dependent relationships between $a^*_\phi(443)$ and ⟨chl⟩.

As the present data set is built up from different cruises in various locations and periods, discerning regional and seasonal trends, if any, is hazardous. In addition, the various cruises cover very distinct ranges of ⟨chl⟩, some of which are rather restricted, which hampers robust cruise-by-cruise relationships to be established. Therefore our purpose here is not to examine the existence of such regional/seasonal relationships. Rather, the aim is to extract general trends for a variety of case 1 waters, to assess the natural variability around these trends, and to evaluate the impact of this variability upon bio-optical modeling.

3.2. Variations of Particulate Absorption in the Near-Surface Layer

With reference to the particular problem of modeling the diffuse reflectance $R(\lambda)$, the analysis of the a_p versus ⟨chl⟩ variations has to be restricted to the layer accessible to remote sensing observations, i.e., the layer corresponding to the first optical depth [*Gordon and McCluney*, 1975]. This depth can be simply computed as $z_e/4.6$, where z_e, the euphotic depth, is either determined from the measured downwelling photosynthetically available radiation (PAR) profile when available or estimated from the vertical profile of ⟨chl⟩ [*Morel*, 1988]. When the data set is restricted to this near-surface layer (260 samples out of 1166), the variations of $a_p(440)$ versus ⟨chl⟩ can be described by the relationship

$$a_p(440) = 0.0519\ \langle \mathrm{chl} \rangle^{0.598}, \qquad r^2 = 0.92 \qquad (4)$$

which does not significantly differ from (1) (Figure 1c). It can also be observed that with the same exceptions as in Figure 1a (samples from EUMELI 4 and some PACIPROD and CHLOMAX samples), the lines corresponding to the prediction interval at the 90% confidence level for the whole data set still represent realistic upper and lower limits for the near-surface layer.

Larger differences between the a_p values within and below the near-surface layer might be expected within the spectral bands of some pigments such as the nonphotosynthetic carotenoids (e.g., zeaxanthin, diatoxanthin, diadinoxanthin), as it is well known that these pigments are more abundant (relative to ⟨chl⟩) within the surface well-lit layer than in deeper waters. As these pigments have a broad absorption band centered on the domain 470–500 nm [e.g., *Bidigare et al.*, 1990], this hypothesis was tested by comparing the $a_p(490)$ versus ⟨chl⟩ relationships for the near-surface layer and for the deeper layer. Somewhat unexpectedly, they were found to be rather close (with $a_p(490) = 0.0330\ \langle \mathrm{chl} \rangle^{0.594}$ for the near-surface layer and $a_p(490) = 0.0345\ \langle \mathrm{chl} \rangle^{0.631}$ for the deeper layer). Similar results are obtained when considering $a_\phi(490)$ instead of $a_p(490)$. This suggests that the nonphotosynthetic pigments influence only weakly the a_p (and a_ϕ) versus ⟨chl⟩ relationships near the surface, probably because the ratio of total (photosynthetic + nonphotosynthetic) carotenoids to ⟨chl⟩ does not vary greatly throughout the euphotic zone (see, e.g., *Allali et al.* [1997] for the OLIPAC cruise).

3.3. Contribution of Nonalgal Particles to Total Particulate Absorption

As suggested by the similarity of the exponents in (1) and (2), the ratio of nonalgal absorption to total particulate absorption at 440 nm, $a_{\mathrm{nap}}(440)/a_p(440)$, does not reveal a regular trend as a function of ⟨chl⟩ (Figure 2a). Waters from the equatorial and subequatorial Pacific (FLUPAC and OLIPAC cruises) exhibit particularly low $a_{\mathrm{nap}}(440)/a_p(440)$ values, mostly between 0.01 and 0.15. In contrast, oligotrophic Mediterranean waters (MINOS cruise) generally show high values for this ratio (up to 0.8). Except for these cases, most of the points lie between 0.15 and 0.60, with a cluster around ~0.25–0.30, whatever the ⟨chl⟩ range, as previously inferred from the comparison between (1) and (2). It could be argued that this rather large variability originates from a varying contribution of nonalgal particles throughout the water column. When restricting the analysis to the first optical depth, however, the range observed above still remains unchanged (Figure 2b).

This range in $a_{\mathrm{nap}}(440)/a_p(440)$ is consistent with that observed for temperate, subtropical, and subpolar regions by *Cleveland* [1995] (approximately 0.2–0.8). This study already emphasized that the proportion of absorption by nonalgal particles exhibited no simple trend as a function of ⟨chl⟩. Note that this author did not observe a particularly low content in nonalgal particles for waters from the equatorial Pacific. In contrast, the a_p spectra that we measured in these waters were close in shape to those of "pure cultures," which indicates that waters were dominated by living phytoplankton [*Allali et al.*, 1997]. Since for these cruises, $a_{\mathrm{nap}}(\lambda)$ was obtained from $a_p(\lambda)$ by numerical decomposition, an artifact could be suspected. During the OLIPAC cruise, however, $a_{\mathrm{nap}}(\lambda)$ was also determined experimentally for several samples, so that it could be confirmed that the low a_{nap} values were not an artifact of the decomposition. It appears therefore that no simple relationship between the contributions of nonalgal particles and phytoplankton to absorption can presently be proposed, which is not surprising, considering the variety and complexity of the

factors controlling interactions between these two components [*Nelson and Robertson*, 1993; see also *Siegel and Michaels*, 1996].

3.4. Spectral Dependence of Absorption by Nonalgal Particles

Absorption by nonalgal particles has long been recognized to vary approximately according to an exponential function of the form [e.g., *Yentsch*, 1962; *Kirk*, 1980; *Roesler et al.*, 1989]:

$$a_{nap}(\lambda) = a_{nap}(\lambda_0) \exp [- S(\lambda - \lambda_0)] \quad (5)$$

This expression is found adequate for the present measurements (Figure 3). For the cruises during which the method of *Kishino et al.* [1985] was applied, the values of the slope S can be determined by fitting $a_{nap}(\lambda)$ to (5). When applying this procedure to the experimental $a_{nap}(\lambda)$ values in the spectral domain 380–700 nm, the coefficient of determination r^2 is higher than 0.90 in most cases (262 out of 267 measured $a_{nap}(\lambda)$ spectra). The S values obtained by numerical decomposition are not considered here, because it was shown previously that, in contrast to the retrieved $a_\phi(\lambda)$ and $a_{nap}(\lambda)$ values, the retrieved S values are sensitive to the assumptions used for the decomposition (see discussion and Figure 9 of *Bricaud and Stramski* [1990]).

The S values estimated from measured a_{nap} spectra range between 0.008 and 0.016 nm^{-1}, with an average value of 0.011 nm^{-1} (standard deviation 0.0025, $N = 267$). Average values of S are 0.012 (±0.002), 0.011 (±0.002), and 0.010 (±0.001) nm^{-1} for each of the three ⟨chl⟩ decades (0.01–0.1, 0.1–1, 1–10 mg m^{-3}), respectively. These values are in good agreement with those reported by *Roesler et al.* [1989] from their measurements off the San Juan Islands (40 spectra), as well as with those they compiled from previously published works (S = 0.011 ± 0.002 nm^{-1} in both cases). The variations in this spectral dependence also show some similarities with CDOM, although the slope values appear to be, on average, lower for nonalgal particles. *Carder et al.* [1989] observed S values for CDOM varying from 0.011 to 0.017 nm^{-1}, with the high values in oligotrophic surface waters, related to a larger fraction of fulvic acids, and the low values in areas of senescent blooms [see also *Green and Blough*, 1994].

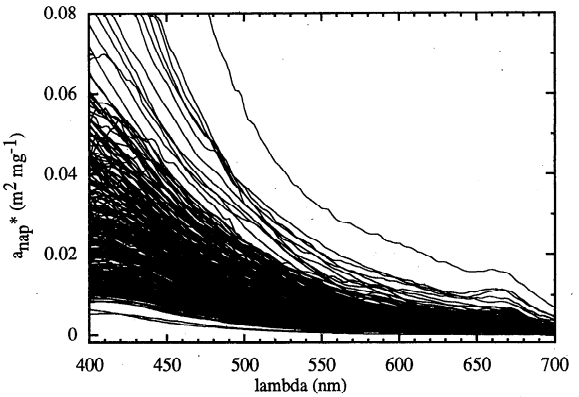

Figure 3. Spectra of the chl-specific absorption coefficient of nonalgal particles, $a^*_{nap}(\lambda)$, obtained using the method of *Kishino et al.* [1985]. All spectra are shown to illustrate the range of variation of a^*_{nap}.

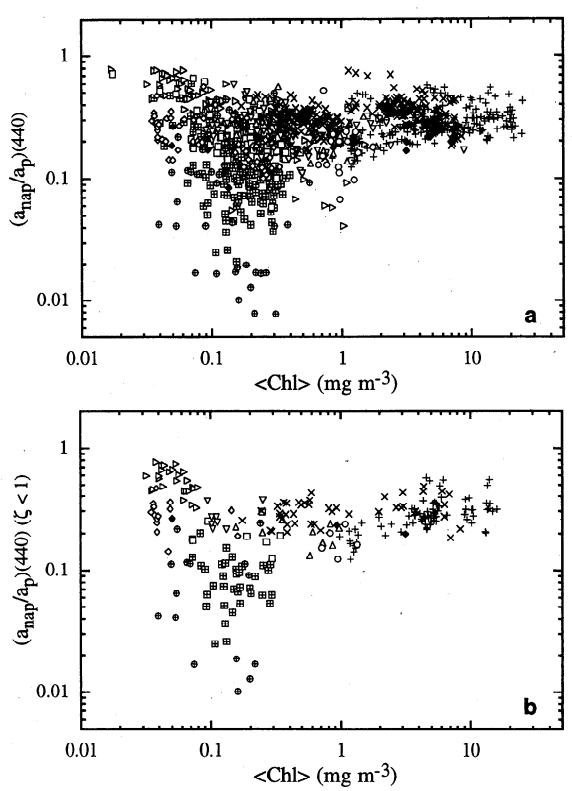

Figure 2. (a) Variations of the ratio of nonalgal absorption to total particle absorption at 440 nm $(a_{nap}/a_p)(440)$ as a function of ⟨chl⟩. Symbols are the same as in Figure 1. (b) Same as Figure 2a, but for the samples located within the first optical depth.

3.5. Parameterization of the Chl-specific Particulate Absorption Spectra

This parameterization consists of fitting the relationship between $a_p(\lambda)$ and ⟨chl⟩ at each wavelength to a power function

$$a_p(\lambda) = A_p(\lambda)^{\langle chl \rangle E_p(\lambda)} \quad (6)$$

which can be transformed into

$$a^*_p(\lambda) = A_p(\lambda)^{\langle chl \rangle E_p(\lambda) - 1} \quad (6')$$

The values of $A_p(\lambda)$, $E_p(\lambda)$, and the coefficients of determination on the log-transformed data r^2 are shown in Figure 4, as compared to those (A_ϕ, E_ϕ) obtained for a_ϕ. The numerical values of these various coefficients (at 2-nm intervals) can be provided on request. Note that A_ϕ and E_ϕ correspond to A and $(1 - B)$ of *Bricaud et al.* [1995, equation (1)]; the numerical values are actually slightly different, as they have been derived from an enlarged data set.

As noted for the 440-nm wavelength, the values of the exponents $E_p(\lambda)$ and $E_\phi(\lambda)$ are very close throughout the 400- to 520-nm domain, indicating again that the contribution of nonalgal particles to total particulate absorption shows no particular trend with ⟨chl⟩. As shown by the coefficients of determination (Figure 4, bottom), the scatter of the a_p versus ⟨chl⟩ relationship is very similar to that of the a_ϕ versus ⟨chl⟩ relationship throughout this wavelength domain. The E_p and E_ϕ values are also in good agreement from 640 to 700 nm. In the green domain, mainly between 520 and 600 nm, they diverge and the E_p values become lower, indicating a stronger nonlinearity.

The difference between the A_p and A_ϕ spectra, very slight

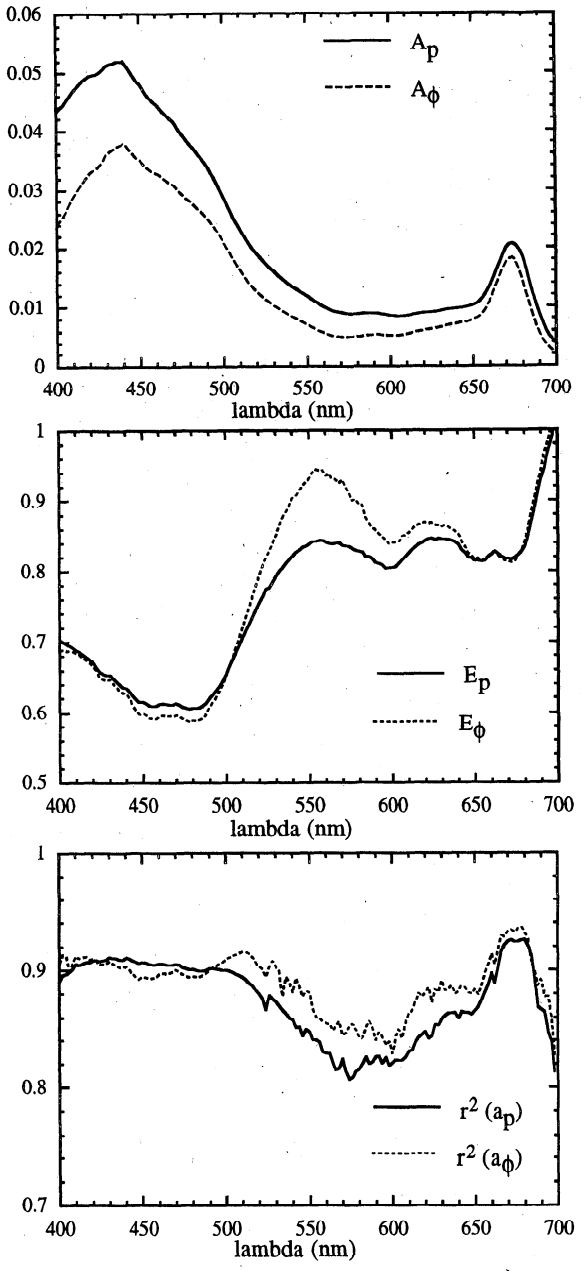

Figure 4. Spectral values of the numerical coefficients (top) A_p and (middle) E_p in the power function representing the variations of $a_p(\lambda)$ as a function of ⟨chl⟩ (equation (6)) and (bottom) coefficients of determination on the log-transformed data, r^2. The corresponding values for the absorption coefficients of living phytoplankton $a_\phi(\lambda)$ are shown as dashed lines for comparison.

within the red absorption band, increases toward the blue domain and expresses, as expected, the increasing contribution of nonalgal particles to total absorption with decreasing wavelength. As the exponents $E_p(\lambda)$ and $E_\phi(\lambda)$ are very close in the blue and red domains, the ratio $A_\phi(\lambda)/A_p(\lambda)$ can be directly used to evaluate the contribution of phytoplankton to particulate absorption at various wavelengths. For the present data set the contribution of algae (found earlier to be 73%, on average, at 440 nm) turns out to be 88% at the red absorption maximum (675 nm) and drops to 55% at 400 nm, where the contribution of nonalgal particles is the highest (Figure 4, top).

Figure 5 shows the mean $a_p^*(\lambda)$ spectra computed for various ⟨chl⟩ values (solid lines) and compared to $a_\phi^*(\lambda)$ spectra (dashed lines), obtained by using the above parameterizations. The higher relative contribution of nonalgal particles at shorter wavelengths is revealed by the slight deformation of the spectral shape of a_p^* compared to a_ϕ^*. It is remarkable, however, that even for very low ⟨chl⟩ values, the shape of the a_p^* spectra remains strongly influenced by phytoplanktonic pigments. This feature may be overemphasized by our data set because of the numerical dominance of Pacific oligotrophic waters, where the contribution of nonalgal particles seems to be exceptionally weak. However, it is believed to be real and consistent with the fact that in most other areas (with the exception of the MINOS cruise), the relative contribution of nonalgal particles to absorption is not higher in oligotrophic waters than in eutrophic waters (Figure 2). Note also the progressive appearance of an absorption shoulder around 590–600 nm when waters become more oligotrophic (decreasing ⟨chl⟩); this feature originates from the increasing occurrence of divinyl-chl *b* present in prochlorophytes.

3.6. Comparison With the Parameterization of the Diffuse Attenuation Coefficient

It is worthwhile examining whether the present parameterization of particulate absorption as a function of ⟨chl⟩ is consistent with that established for the diffuse attenuation coeffi-

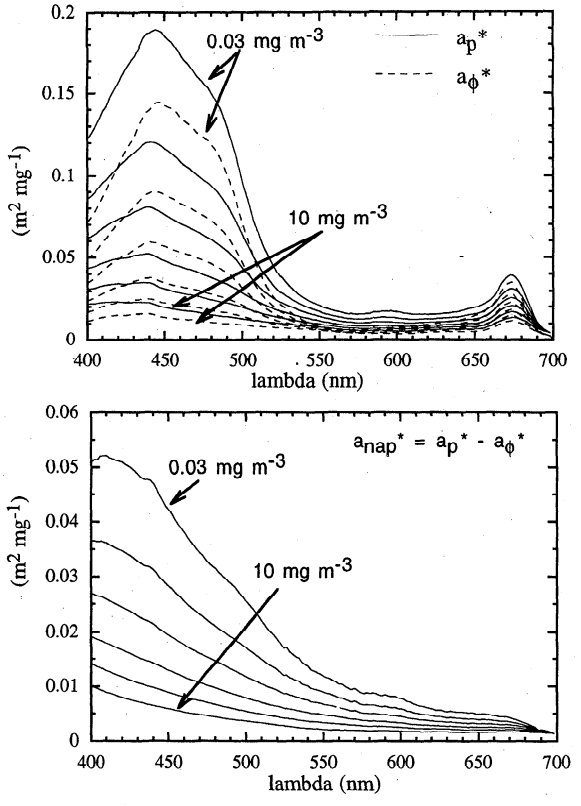

Figure 5. Chlorophyll-specific absorption spectra of particles $a_p^*(\lambda)$ (solid lines) for various values of ⟨chl⟩ (0.03, 0.1, 0.3, 1, 3, and 10 mg m^{-3}), as reconstructed from (6′), with the spectral values of A_p and E_p displayed in Figure 4. The corresponding spectra for living phytoplankton, $a_\phi^*(\lambda)$ (top, dashed lines) and the difference spectra ($a_{\text{nap}}^* = a_p^* - a_\phi^*$) (bottom) are also shown.

cient for downwelling irradiance $K_d(\lambda)$ by *Morel* [1988]. This former parameterization,

$$K_d(\lambda) = K_w(\lambda) + \chi(\lambda)\,\langle \mathrm{chl}\rangle^{e(\lambda)} \qquad (7)$$

where K_w represents the diffuse attenuation coefficient of pure seawater, was based on a statistical analysis of $K_d(\lambda)$ values derived from downwelling irradiance spectra. Therefore the experimental methods used for providing $K_d(\lambda)$ and $a_p(\lambda)$ are completely different. The data sets are also almost independent, from a geographical viewpoint, as only the PACIPROD cruise is included in both data sets (21 out of the 175 K_d spectra, 30 out of the 1166 a_p spectra). On the basis of the same approach, a new statistical analysis that includes also the K_d measurements acquired during the cruises EUMELI 3, EUMELI 4, OLIPAC and MINOS (207 additional spectra) was recently performed (A. Morel et al., manuscript in preparation, 1998), and led to a new set of coefficients for (7). The two sets (actually rather close) are used simultaneously below.

To examine whether the parameterizations of a_p and K_d are consistent, we have computed $K_d(\lambda)$ from $a(\lambda)$ and $b(\lambda)$, using an empirical formula derived by *Kirk* [1981]. This computation is described in the appendix. The K_d values computed in this way can then be compared with those parameterized by *Morel* [1988] and A. Morel et al. (manuscript in preparation, 1998). Such a comparison was already attempted by *Morel* [1988]; however, for lack of available data, the chl-specific absorption coefficients of phytoplankton were assumed to be independent of ⟨chl⟩, and the contributions of nonalgal particles and CDOM were ignored. Here the same approach can be used again in a more realistic way.

Since for very low ⟨chl⟩, the K_d values are governed almost exclusively by pure seawater, a more meaningful comparison is performed by examining the differences $(K_d - K_w)(\lambda) = K_{\mathrm{bio}}(\lambda)$. The K_{bio} spectra provided by both approaches have been compared for three ⟨chl⟩ values (Figure 6). For low and moderate ⟨chl⟩ values (0.1 and 1 mg m^{-3}) the spectral shape is reasonably well reproduced throughout the spectrum, except below 440 nm, and in the 560- to 620-nm domain. It is recalled that the spectral values of a_p have to be considered with caution in the green part of the spectrum because of the low coefficients of determination (see Figure 4). For high ⟨chl⟩ values (10 mg m^{-3}) the reconstructed values below 500 nm become significantly lower than those provided by (7); also, the blue maximum tends to disappear (especially in the presence of CDOM), while it remains visible on the spectrum provided by (7). The values in the red part of the spectrum (around 670 nm) are in good agreement, not only for low ⟨chl⟩ values, where water absorption predominates, but also for ⟨chl⟩ values as high as 10 mg m^{-3}.

In spite of the spectral divergences noted above, it is important to note that, over the whole ⟨chl⟩ range, the K_{bio} values experience a variation by a factor of about 20 and that these variations in amplitude are correctly reproduced by (10)–(13). This agreement between the absolute values is comforting; the present uncertainty concerning the actual contribution of CDOM to total absorption prevents further progress in the comparison. It can be concluded, however, that the parameterizations of $K_d(\lambda)$ and $a_p(\lambda)$ are basically consistent for a ⟨chl⟩ range covering oligotrophic to eutrophic waters.

3.7. Implications for Diffuse Reflectance Modeling

3.7.1. Impact of the variations in absorption. Models aimed at predicting ocean color from water content generally rely upon unique relationships between absorption (or diffuse attenuation), scattering, and ⟨chl⟩. It is therefore necessary to examine how the natural variability in a_p may affect the diffuse reflectance of the ocean. With this purpose a simple reflectance model was operated, using the relationship

$$R(\lambda) = f\{0.5 b_w(\lambda) + [b_{\tilde{b}p}(\lambda)\, b_p(\lambda)]\}/a(\lambda) \qquad (8)$$

where $(b_{\tilde{b}p}/b_p)$ represents the backscattering efficiency of particles; f is the proportionality factor between R and the backscattering-to-absorption ratio and varies with the ⟨chl⟩ content, the Sun elevation, and wavelength [*Morel and Gentili*, 1996]. The model was operated here with the Sun at zenith. The $a(\lambda)$ coefficients were computed using (11) and (12) (see appendix); y in (12) was given the value 0.2, and the $a_p(\lambda)$ coefficients

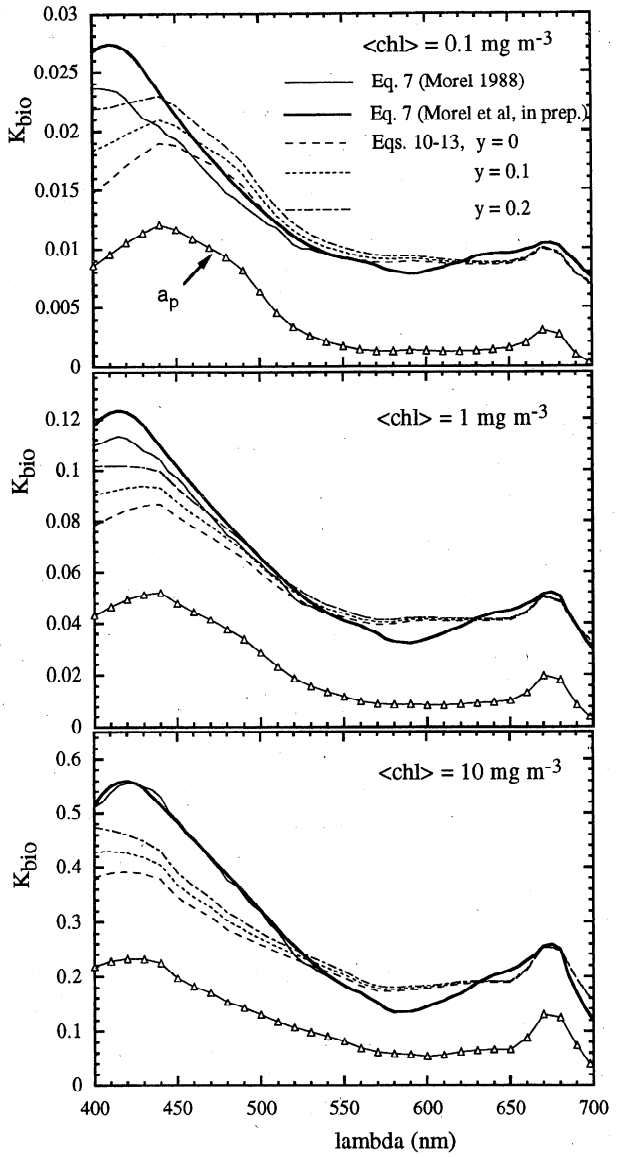

Figure 6. Comparison of the nonwater diffuse attenuation spectra (K_{bio} (in m^{-1}) obtained by using (7) with two sets of numerical coefficients (solid lines) and (10)–(13) (dashed and dotted lines), for three values of the chlorophyll concentration. The y values indicated are those used in (12). The a_p spectra provided by (6) for the same chlorophyll concentrations are also shown for comparison.

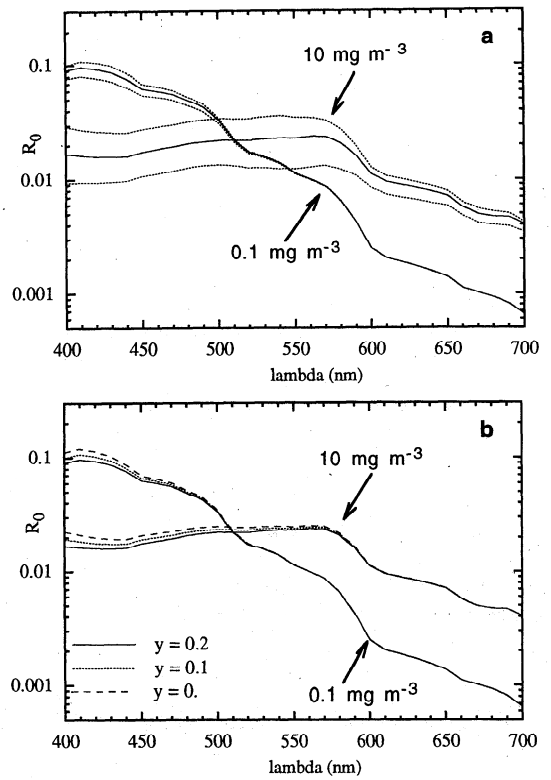

Figure 7. Reflectance spectra for a null depth and for a Sun at zenith, modeled using (8) and (11)–(13) for two ⟨chl⟩ values and (a) using the mean a_p versus ⟨chl⟩ relationships in (11) (solid lines) and the upper and lower limits of these relationships, estimated by computing at each wavelength the prediction intervals at a 90% confidence level (dotted lines), and (b) using the mean relationships a_p versus ⟨chl⟩ in (11) and assuming various contributions of locally produced colored dissolved organic matter (CDOM) to total absorption (various y values in (12)).

were parameterized as in (6). The numerical coefficients $A_p(\lambda)$ and $E_p(\lambda)$ computed for the whole euphotic zone were preferred to those obtained for only the near-surface layer (they are not statistically different and are thought to be more robust because they are derived from a fourfold larger data set). The particle scattering coefficient $b_p(\lambda)$ was computed by applying (13) and (13′) and subtracting the molecular scattering coefficients $b_w(\lambda)$. Finally, the particle backscattering efficiency, (b_{bp}/b_p), was made varying with ⟨chl⟩ as in the paper by *Morel* [1988].

In order to assess the impact of the residual variability in $a_p(\lambda)$ (with respect to the mean $a_p(\lambda)$ versus ⟨chl⟩ relationships), the reflectance spectra were also computed using the upper and lower limits of these coefficients (defined as previously from the prediction intervals at a 90% confidence level). This computation was performed for two values of ⟨chl⟩, 0.1 and 10 mg m^{-3} (Figure 7a). As expected, the impact of this variability is rather limited at low ⟨chl⟩, where molecular absorption predominates. It becomes much higher at high ⟨chl⟩, about a factor of 3 over the blue-green domain, for 10 mg m^{-3}. In the red part of the spectrum this effect is again partially masked by the increasing contribution of water absorption.

For the sake of comparison, the effect of the possible changes in the CDOM concentration has been examined (Figure 7b). The absorption coefficient at 440 nm, a_{ds} (440), was varied as previously, from 0 to 20% of the $(a_w + a_p)(440)$ coefficient (equation (12)). At low ⟨chl⟩ (0.1 mg m^{-3}) the changes in CDOM absorption and variability in particulate absorption appear to have a similar impact upon reflectance (limited essentially to the blue wavelengths). At high ⟨chl⟩ (10 mg m^{-3}) the effect of changing CDOM absorption becomes negligible compared to the effect of variability in particulate absorption.

3.7.2. Impact of the combined variations in absorption and scattering. The above computations assume that particle scattering at 660 nm follows perfectly (13′). In reality, the $b_p(660)$ values also show natural variability around this mean relationship [see *Loisel and Morel*, 1998], comparable to that observed for particulate absorption. Therefore it is of interest to know whether deviations of particulate absorption (with respect to the a_p value provided by the parameterization) are associated or not to deviations in particle scattering or, in other words, whether variations in a_p and b_p might counterbalance or conversely cumulate their effects upon reflectance.

This was examined for the cruises where simultaneous measurements of $a_p(\lambda)$ and the attenuation coefficient at 660 nm, $c(660)$ (measured in situ with a Sea Tech transmissometer [*Bartz et al.*, 1978]) were available. The $c(660)$ values were corrected for pure seawater attenuation by subtracting the deep local value [see *Loisel and Morel*, 1998] and then converted into $b_p(660)$ by subtracting the measured $a_p(660)$ value (in general, a few percent of the $c(660)$ value). For each station and depth the relative deviations (in percent) of $b_p(660)$ and $a_p(440)$ from their average value were computed as:

$$\delta b_p(660) = 100[b_p(660) - b_{pm}(660)]/b_{pm}(660) \quad (9)$$

$$\delta a_p(440) = 100[a_p(440) - a_{pm}(440)]/a_{pm}(440) \quad (9')$$

where $b_{pm}(660)$ and $a_{pm}(440)$ were obtained using (13′) and (1), respectively (note that $\delta b_p(660)$ values close to −100% correspond to samples at the bottom of the euphotic zone, where $b_p(660)$ approaches 0).

Figure 8, divided in four panels, demonstrates that several situations occur. (1) In panels I and II, where $\delta b_p(660)$ and $\delta a_p(440)$ are of identical sign, low and high a_p values are associated with low and high b_p values, respectively. Therefore their variations should partially compensate for each other (totally for those samples lying on the 1:1 line in Figure 8) and should have a limited impact upon diffuse reflectance (provided that there is no change in the backscattering efficiency for these samples). This is the case for most samples of the OLIPAC cruise, as well as some from EUMELI 3, EUMELI 4, and MINOS. For most samples from the OLIPAC cruise the "low b_p–low a_p" values (with respect to the mean values) are easily explained by their exceptionally low content in nonalgal particles. On the opposite side, the "high b_p–high a_p" values observed during the MINOS cruise (corresponding mainly to surface samples) indicate a high detrital content comparatively to ⟨chl⟩. (2) in Panels III and IV, in contrast, the deviations in a_p and b_p are opposite (low and high a_p values are associated to high and low b_p values, respectively). In such situations the effects of variations in a_p and b_p upon diffuse reflectance are cumulative and should induce reflectance variations still larger than those predicted in Figure 7a. This is the case for some EUMELI 3 and OLIPAC samples and for most MINOS and EUMELI 4 samples. For those samples the high $a_p(440)$ values mainly result from the pigment composition, as also demonstrated by the high $a_\Phi(440)$ values (not shown; see

Babin et al. [1996] for EUMELI 4). This particular pigment composition (abundance of zeaxanthin) has no direct effect on $b_p(660)$, but it may indicate the presence of phytoplanktonic populations of small size, such as prochlorophytes, which are characterized by very low chl-specific scattering coefficients [*Morel et al.*, 1993].

With regard to the diversity of these situations, the variability shown in Figure 7a may probably be considered as realistic, to the extent that variations in a_p are very seldom compensated by those in b_p. These results emphasize the difficulty of relying upon the absolute values of reflectance, when, for instance, attempting to retrieve the chlorophyll content from satellite data via a semianalytical reflectance model. Even when ignoring other sources of uncertainty in reflectance models, such as the spectral dependence of particle scattering, the variations of the backscattering efficiency with the ⟨chl⟩ content, and the contribution of CDOM to total absorption, the unexplained variability in $a_p(\lambda)$ and $b_p(\lambda)$ may be responsible for large variations in the amplitude of reflectance, particularly for moderate or high chlorophyll contents.

Reflectance values, however, do not vary in an erratic way from one wavelength to the other, as demonstrated, for instance, by the positive correlation between $\delta a_p(440)$ and $\delta a_p(550)$ (Figure 9, panels I and II). This emphasizes the interest of using reflectance ratios instead of absolute values of reflectance when retrieving the chlorophyll concentration from satellite data. In such algorithms the impact of the variability in a_p upon the chlorophyll retrieval is significantly reduced (actually cancelled for the samples on the 1:1 line in Figure 9). It is observed in Figure 9, however, that for a nonnegligible number of samples (panels III and IV), some low/high values of $a_p(440)$ coexist with high/low values of $a_p(550)$. In such cases the impact of the variations in particulate absorption is obviously not reduced when using reflectance ratios.

4. Conclusions

The former analysis of the natural variations in absorption by phytoplankton [*Bricaud et al.*, 1995] was performed mainly in view of modeling primary production, and its results were accounted for in a revised version of the photophysiological parameters involved in such a modeling [*Morel et al.*, 1996]. The present analysis dealing with total particulate absorption is mainly aimed at providing an input parameter for modeling apparent optical properties, such as diffuse attenuation or reflectance. It also assesses the respective contributions of algal and nonalgal particles to particulate absorption in waters with various trophic regimes.

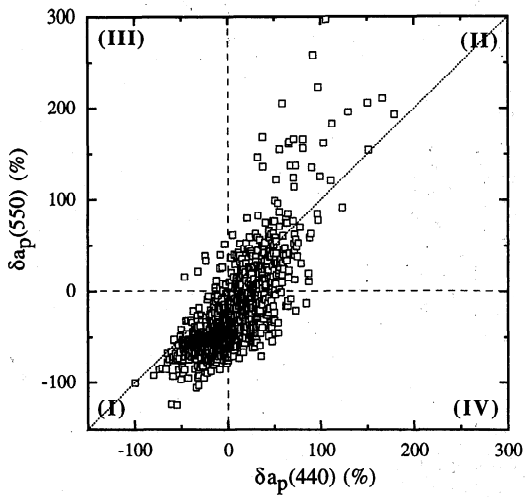

Figure 9. Relationship between the deviations of the particulate absorption coefficients at 440 and 550 nm, $\delta a_p(440)$ and $\delta a_p(550)$, respectively, from their respective average values.

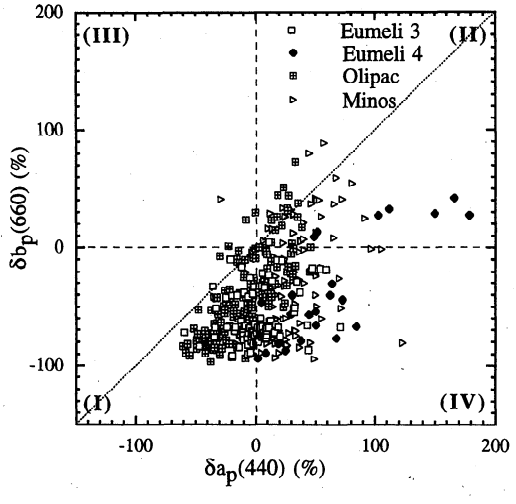

Figure 8. Relationship between the deviation of the particulate scattering coefficient at 660 nm from its average value, $\delta b_p(660)$, in percent (equation (9)), and the deviation of the particulate absorption coefficient from its average value, $\delta a_p(440)$, in percent (equation (9′)).

Both parameterizations (for a_p and a_ϕ) should be used only when bearing in mind their limitations: (1) they are applicable to case 1 waters only and not valid outside the ⟨chl⟩ range corresponding to the present data set; (2) because of the large possible individual deviations from the average relationships, they can in no way be operated on a sample-by-sample basis; and (3) in spite of the rather large data set, these parameterizations are not intended to be universal, in particular, because some peculiar situations (e.g., polar waters) have not been explored, and the data set was not appropriate to detect regional or seasonal trends, if any.

The present analysis demonstrates that the $a_p^*(\lambda)$ coefficients can vary by more than 1 order of magnitude when the chl *a* concentration varies by 3 orders of magnitude (0.02 to 25 mg m^{-3}). Such variations definitely have to be taken into account when developing analytical (or semianalytical) bio-optical models. The actual impact of these variations upon diffuse reflectance values, for instance, is predictable; however, two other input parameters in reflectance models, absorption by CDOM and particle backscattering efficiency, still remain very poorly documented. While the GF/F technique for particulate absorption measurements has been widely used during the last decade, so that this parameter is now rather well known, absorption by CDOM and particle backscattering was very seldom determined at sea because of instrumental limitations. The development and increasing use of new in situ optical devices such as spectral absorption meters [*Bruce et al.*, 1996] equipped with filters and backscattering sensors [*Maffione and Dana*, 1997] should improve the situation.

As a first approximation, the nonlinear a_p versus ⟨chl⟩ and a_ϕ versus ⟨chl⟩ relationships parallel each other, indicating that the contribution of nonalgal particles to total absorption oscil-

lates around an average value (~25–30%), whatever the chlorophyll content in case 1 waters. This does not contradict the findings of previous studies showing that the carbon-to-⟨chl⟩ ratio increases with decreasing ⟨chl⟩ [*Hobson et al.*, 1973; *Loisel and Morel*, 1998], but this indicates that the increase in this ratio is not necessarily reflected by a relative increase in nonalgal absorption.

The contribution of nonalgal absorption to total absorption actually exhibits large variations around its average value and also shows exceptionally low values in some areas (e.g., in the equatorial Pacific); therefore modeling optical properties for the nonalgal compartment remains uncertain. As the scatter observed on the $a_p(\lambda)$ versus ⟨chl⟩ relationships is not higher than that for a_ϕ, it appears that, at least as a first step, absorption by particles can be represented globally in bio-optical models (i.e., without increasing the level of complexity by modeling separately the absorption coefficients of the algal and nonalgal compartments).

The residual variability in particulate absorption (as well as in phytoplanktonic absorption), with respect to the average relationships, is rather large and probably conceals specific and valuable information. Further work is needed to analyze this information. In our present state of knowledge this variability represents a limitation for reflectance prediction, especially because deviations in a_p are generally not compensated by concomitant deviations in particle scattering, so that the amplitude of reflectance is affected. Using spectral reflectance ratios, instead of absolute values of reflectance, greatly cancels out this limitation.

Appendix

Examining whether the parameterizations of $a_p(\lambda)$ and $K_d(\lambda)$ are consistent implies that the contributions to K_d of absorption by CDOM and particle scattering are accounted for. For this we used the approximative formula proposed by *Kirk* [1981]:

$$K_d = (a^2 + 0.256\, ab)^{0.5} \tag{10}$$

where a and b, the total absorption and scattering coefficients, respectively, and K_d are represented at the midpoint of the euphotic zone. Note that this simplified formula does not account for the influence of Sun elevation. The total absorption coefficient is expressed as

$$a(\lambda) = a_w(\lambda) + a_p(\lambda) + a_{ds}(440)\, \exp\,[-0.014(\lambda - 440)] \tag{11}$$

in which $a_w(\lambda)$ is the absorption coefficient of pure seawater [*Pope and Fry*, 1997]. The term $a_{ds}(440)$ exp $[-0.014\ (\lambda - 440)]$ represents absorption by locally produced CDOM, which decreases exponentially with wavelength, with an average slope of −0.014 [*Bricaud et al.*, 1981]. The contribution of CDOM to total absorption is not well documented. *Prieur and Sathyendranath* [1981] suggested that the absorption coefficient of nonalgal matter at 440 nm contributes 20% of the total absorption coefficient at this wavelength. However, this amount included the contribution of nonalgal particles, so that the actual contribution of dissolved yellow substance is probably lower. A review of existing measurements for oceanic waters [*Kirk*, 1994] shows that the absorption coefficient of yellow substance at 440 nm varies roughly from ~0 to 0.1 m^{-1} from clear to eutrophic waters and is likely to vary for a given particulate content. Here the absorption coefficient of CDOM at 440 nm was tentatively represented as

$$a_{ds}(440) = y[(a_w + a_p)(440)] \tag{12}$$

with $y = 0$, 0.1 or 0.2, so that it is allowed to increase with the total absorption coefficient at various rates; the inclusion of a_w implies that a CDOM "background" remains, even in the clearest waters. The total scattering coefficient was represented as

$$b(\lambda) = b_w(\lambda) + [b_p(660)(660/\lambda)] \tag{13}$$

with

$$b_p(660) = 0.252\ \langle \text{chl} \rangle^{0.635} \tag{13'}$$

in which $b_w(\lambda)$ is the scattering coefficient of pure seawater. Equation (13′) was derived by *Loisel and Morel* [1998] from a statistical analysis of 610 recent measurements of in situ attenuation within the upper homogeneous layer (their set 2 and 3); the second part of the bracketed term in (13) makes particle scattering spectrally varying as λ^{-1} [e.g., *Gordon and Morel*, 1983]. The b_w coefficients are those provided by *Morel* [1974]. Note that for the range of ⟨chl⟩ values examined in the comparison (0.1–10 mg m^{-3}; see Figure 6), the ratio b/a, as provided by (11)–(13), varies from 3 to 15, which is in the domain of the validity of (10) ($b/a < 30$).

Notation

Some of these notations differ from those used by *Bricaud et al.* [1995] in order to conform with those recommended by the Joint Global Ocean Flux Study Task Team for Photosynthetic Measurements [*Sakshaug et al.*, 1997].

λ	wavelength, nm.
⟨chl⟩	(chlorophyll a + divinyl chl a + pheophytin a) concentration, mg m^{-3}.
a	absorption coefficient of the water body, m^{-1}.
a_w	absorption coefficient of pure seawater, m^{-1}.
a_p	absorption coefficient of particles, m^{-1}.
a_ϕ	absorption coefficient of living phytoplankton, m^{-1}.
a_{nap}	absorption coefficient of nonalgal particles, m^{-1}.
a_{ds}	absorption coefficient of colored dissolved organic matter, m^{-1}.
a_p^*, a_ϕ^*, a_{nap}^*	chl-specific absorption coefficients, $m^2\ mg^{-1}$.
S	slope of the exponential function representing the spectral dependence of a_{nap} (equation (5)), nm^{-1}.
A_p, E_p	numerical constants in the a_p versus ⟨chl⟩ relationship (equation (6)).
A_ϕ, E_ϕ	numerical constants in the a_ϕ versus ⟨chl⟩ relationship.
K_d	diffuse attenuation coefficient (for downwelling irradiance), m^{-1}.
K_w	diffuse attenuation coefficient of pure seawater, m^{-1}.
K_{bio}	Nonwater diffuse attenuation coefficient ($=K_d - K_w$), m^{-1}.
b	scattering coefficient of the water body, m^{-1}.
b_w	scattering coefficient of pure seawater, m^{-1}.
b_p	scattering coefficient of particles, m^{-1}.

b_b backscattering coefficient of the water body, m^{-1}.
b_{bw} backscattering coefficient of pure seawater, m^{-1}.
b_{bp} backscattering coefficient of particles, m^{-1}.
$\tilde{b}_{bp}$ backscattering efficiency of particles.
R diffuse reflectance.
f proportionality factor between R and b_b/a.
δa_p relative deviation of a_p from its average value, %.
δb_p relative deviation of b_p from its average value, %.
z depth, m.
z_e euphotic depth, m.
ζ optical depth ($=4.6\ z/z_e$).

Acknowledgments. This study was supported by Centre National de la Recherche Scientifique (URA 2076 and GDR 869) and by INSU, ORSTOM, and IFREMER for the cruises that were part of JGOFS FRANCE operations (TOMOFRONT, EUMELI, FLUPAC, and OLIPAC). Data from the LIDAR cruises were acquired through programs of the Maurice Lamontagne Institute and Groupe Interuniversitaire de recherches océanographiques du Québec (GIROQ). The authors wish to thank the chief scientists and crews of the different cruises during which these data were collected. We are grateful to J. Neveux for pigment measurements during the CHLOMAX cruise; to D. Stramski for his contribution to the same cruise; and to F. Vidussi, C. Cailliau, and J. C. Marty for their participation in HPLC measurements. Three anonymous referees are acknowledged for thorough comments. This work is a contribution to the JGOFS France program PROSOPE.

References

Allali, K., A. Bricaud, M. Babin, A. Morel, and P. Chang, A new method for measuring spectral absorption coefficients of marine particles, *Limnol. Oceanogr.*, *40*, 1526–1532, 1995.

Allali, K., A. Bricaud, and H. Claustre, Spatial variations in the chlorophyll-specific absorption coefficients of phytoplankton and photosynthetically active pigments in the equatorial Pacific, *J. Geophys. Res.*, *102*, 12,413–12,423, 1997.

Babin, M., A. Morel, H. Claustre, A. Bricaud, Z. Kolber, and P. G. Falkowski, Nitrogen- and irradiance-dependent variations of the maximum quantum yield of carbon fixation in eutrophic, mesotrophic and oligotrophic marine systems, *Deep Sea Res., Part I*, *43*, 1241–1272, 1996.

Baker, K. S., and R. C. Smith, Bio-optical classification and model of natural waters, II, *Limnol. Oceanogr.*, *27*, 500–509, 1982.

Bartz, R., J. R. V. Zaneveld, and H. Pak, A transmissometer for profiling and moored observations in water, in Ocean Optics V, *Proc. SPIE Int. Soc. Opt. Eng.*, *160*, 102–108, 1978.

Bidigare, R. R., M. E. Ondrusek, J. H. Morrow, and D. A. Kiefer, *In vivo* absorption properties of algal pigments, in Ocean Optics X, *Proc. SPIE Int. Soc. Opt. Eng.*, *1302*, 290–302, 1990.

Bricaud, A., and D. Stramski, Spectral absorption coefficients of living phytoplankton and nonalgal biogenous matter: A comparison between the Peru upwelling area and Sargasso Sea, *Limnol. Oceanogr.*, *35*, 562–582, 1990.

Bricaud, A., A. Morel, and L. Prieur, Absorption by dissolved organic matter of the sea (yellow substance) in the UV and visible domains, *Limnol. Oceanogr.*, *26*, 43–53, 1981.

Bricaud, A., M. Babin, A. Morel, and H. Claustre, Variability in the chlorophyll-specific absorption coefficients of natural phytoplankton: Analysis and parameterization, *J. Geophys. Res.*, *100*, 13,321–13,332, 1995.

Bruce, E. J., M. Borgerson, C. Moore, and A. Weidemann, Hi-Star: A spectrophotometer for measuring the absorption and attenuation of natural waters *in situ* and in the laboratory, in Ocean Optics XIII, *Proc. SPIE Int. Soc. Opt. Eng.*, *2963*, 637–642, 1996.

Carder, K. L., R. G. Steward, G. R. Harvey, and P. B. Ortner, Marine humic and fulvic acids: Their effects on remote sensing of ocean chlorophyll, *Limnol. Oceanogr.*, *34*, 68–81, 1989.

Carder, K. L., S. K. Hawes, K. A. Baker, R. C. Smith, R. G. Steward, and B. G. Mitchell, Reflectance model for quantifying chlorophyll *a* in the presence of productivity degradation products, *J. Geophys. Res.*, *96*, 20,599–20,611, 1991.

Cleveland, J. S., Regional models for phytoplankton absorption as a function of chlorophyll *a* concentration, *J. Geophys. Res.*, *100*, 13,333–13,344, 1995.

Garver, S., D. A. Siegel, and B. G. Mitchell, Variability in near-surface particulate absorption spectra: What can a satellite ocean color imager see?, *Limnol. Oceanogr.*, *39*, 1349–1367, 1994.

Gordon, H. R., and W. R. McCluney, Estimation of the depth of sunlight penetration in the sea for remote sensing, *Appl. Opt.*, *14*, 413–416, 1975.

Gordon, H. R., and A. Morel, Remote assessment of ocean color for interpretation of satellite visible imagery: A review, in *Lecture Notes on Coastal and Estuarine Studies*, vol. 4, 114 pp., Springer-Verlag, New York, 1983.

Gordon, H. R., O. B. Brown, and M. M. Jacobs, Computed relationships between the apparent and inherent optical properties of a flat homogeneous ocean, *Appl. Opt.*, *14*, 417–427, 1975.

Gordon, H. R., O. B. Brown, R. H. Evans, J. W. Brown, R. C. Smith, K. S. Baker, and D. K. Clark, A semianalytic radiance model of ocean color, *J. Geophys. Res.*, *93*, 10,909–10,924, 1988.

Green, S. A., and N. V. Blough, Optical absorption and fluorescence properties of chromophoric dissolved organic matter in natural waters, *Limnol. Oceanogr.*, *39*, 1903–1916, 1994.

Hobson, L. A., D. W. Menzel, and R. T. Barber, Primary productivity and the sizes of the pools of organic carbon in the mixed layer of the ocean, *Mar. Biol.*, *19*, 298–306, 1973.

Kirk, J. T. O., Spectral absorption properties of natural waters: Contribution of the soluble and particulate fractions to light absorption in some inland waters of south-eastern Australia, *Aust. J. Mar. Freshwater Res.*, *31*, 287–296, 1980.

Kirk, J. T. O., Monte Carlo study of the nature of the underwater light field in, and the relationships between optical properties of, turbid yellow waters, *Aust. J. Mar. Freshwater Res.*, *32*, 517–532, 1981.

Kirk, J. T. O., *Light and Photosynthesis in Aquatic Ecosystems*, Cambridge Univ. Press, New York, 1994.

Kishino, M., M. Takahashi, N. Okami, and S. Ichimura, Estimation of the spectral absorption coefficients of phytoplankton in the sea, *Bull. Mar. Sci.*, *37*, 634–642, 1985.

Le Borgne, R., and H. Gesbert (Eds.), Campagne océanographique FLUPAC à bord du N. O. l'ATALANTE, 23 septembre au 29 octobre 1994, Recueil de données. Arch. Sci. de la Mer, Océanogr., *2*, 330 pp., Off. de la Rech. Sci. et Tech. d'Outre-Mer, Nouméa, New Caledonia, 1995.

Loisel, H., and A. Morel, Light scattering and chlorophyll concentration in Case I waters: A reexamination, *Limnol. Oceanogr.*, *43*, 847–858, 1998.

Maffione, R. A., and D. R. Dana, Instruments and methods for measuring the backward-scattering coefficient of ocean waters, *Appl. Opt.*, *36*, 6057–6067, 1997.

Mitchell, B. G., and O. Holm-Hansen, Bio-optical properties of Antarctic Peninsula waters: Differentiation from temperate ocean models, *Deep Sea Res., Part A*, *38*, 1009–1028, 1991.

Mitchell, B. G., and D. A. Kiefer, Variability in pigment specific particulate fluorescence and absorption spectra in the northeastern Pacific Ocean, *Deep Sea Res., Part A*, *35*, 665–689, 1988.

Mobley, C., *Light and Water: Radiative Transfer in Natural Waters*, 592 pp., Academic, San Diego, Calif., 1994.

Morel, A., Optical properties of pure water and pure seawater, in *Optical Aspects of Oceanography*, edited by N. G. Jerlov, pp. 1–24, Academic, San Diego, Calif., 1974.

Morel, A., Optical modeling of the upper ocean in relation to its biogenous matter content (Case I waters), *J. Geophys. Res.*, *93*, 10,749–10,768, 1988.

Morel, A., Consequences of a *Synechococcus* bloom upon the optical properties of oceanic (Case 1) waters, *Limnol. Oceanogr.*, *42*, 1746–1754, 1997.

Morel, A., and B. Gentili, Diffuse reflectance of oceanic waters, III, Implication of bidirectionality for the remote sensing problem, *Appl. Opt.*, *35*, 4850–4862, 1996.

Morel, A., Y. H. Ahn, F. Partensky, D. Vaulot, and H. Claustre, *Prochlorococcus* and *Synechococcus*: A comparative study of their optical properties in relation to their size and pigmentation, *J. Mar. Res.*, *51*, 617–649, 1993.

Morel, A., D. Antoine, M. Babin, and Y. Dandonneau, Measured and modeled primary production in the northeast Atlantic (EUMELI JGOFS program): The impact of natural variations in photosynthetic parameters on model predictive skill, *Deep Sea Res., Part I, 43*, 1273–1304, 1996.

Morrow, J. H., D. A. Kiefer, and W. S. Chamberlin, A two-component description of spectral absorption by marine particles, *Limnol. Oceanogr., 34*, 1500–1509, 1989.

Moutin, T., and B. Coste (Eds.), Campagne océanographique OLIPAC à bord du N. O. l'ATALANTE, 3 novembre-1er décembre 1994, Recueil des données, report, 266 pp., Joint Global Ocean Flux Study, Inst. Fr. de Rech. pour l'Exploitation de la Mer, Inst. Natl. des Sci. de l'Univers, Marseille, France, 1996.

Nelson, J. R., and S. Guarda, Particulate and dissolved spectral absorption on the continental shelf of the southeastern United States, *J. Geophys. Res., 100*, 8715–8732, 1995.

Nelson, J. R., and C. Y. Robertson, Detrital spectral absorption: Laboratory studies of visible light effects on phytodetritus absorption, bacterial spectral signal, and comparison to field measurements, *J. Mar. Res., 51*, 181–207, 1993.

Pope, R. M., and E. S. Fry, Absorption spectrum (380–700 nm) of pure water, II, Integrating cavity measurements, *Appl. Opt., 36*, 8710–8723, 1997.

Preisendorfer, R. W., *Application of Radiative Transfer Theory to Light Measurements in the Sea, Monogr. 10*, pp. 11–30, Int. Union of Geod. and Geophy., Paris, 1961.

Prieur, L., and S. Sathyendranath, An optical classification of coastal and oceanic waters based on the specific spectral absorption curves of phytoplankton pigments, dissolved organic matter, and other particulate materials, *Limnol. Oceanogr., 26*, 671–689, 1981.

Roesler, C. S., M. J. Perry, and K. L. Carder, Modeling in situ phytoplankton absorption from total absorption spectra in productive inland marine waters, *Limnol. Oceanogr., 34*, 1510–1523, 1989.

Sakshaug, E., A. Bricaud, Y. Dandonneau, P. G. Falkowski, D. A. Kiefer, L. Legendre, A. Morel, J. Parslow, and M. Takahashi, Parameters of photosynthesis: definitions, theory and interpretation of results, *J. Plankton Res., 19*, 1637–1670, 1997.

Siegel, D. A., and A. F. Michaels, Quantification of non-algal light attenuation in the Sargasso Sea: Implications for biogeochemistry and remote sensing, *Deep Sea Res., Part II, 43*, 321–345, 1996.

Smith, R. C., and K. S. Baker, Optical classification of natural waters, *Limnol. Oceanogr., 23*, 260–267, 1978.

Trüper, H. G., and C. S. Yentsch, Use of glass-fiber filters for the rapid preparation of in vivo absorption spectra of photosynthetic bacteria, *J. Bact., 94*, 1255–1256, 1967.

Vidussi, F., H. Claustre, J. Bustillos-Guzman, C. Cailliau, and J. C. Marty, Rapid HPLC method for determination of phytoplankton chemotaxinomic pigments: Separation of chlorophyll *a* from divinyl-chlorophyll *a*, and zeaxanthin from lutein, *J. Plankton Res., 18*, 2377–2382, 1996.

Yentsch, C. S., Measurement of visible light absorption by particulate matter in the ocean, *Limnol. Oceanogr., 7*, 207–217, 1962.

Yentsch, C. S., and D. A. Phinney, A bridge between ocean optics and microbial ecology, *Limnol. Oceanogr., 34*, 1694–1705, 1989.

K. Allali, M. Babin, A. Bricaud, H. Claustre, and A. Morel, Laboratoire de Physique et Chimie Marines, Université Pierre et Marie Curie and CNRS, BP8, 06238 Villefranche-sur-Mer Cedex, France. (annick@ccrv.obs-vlfr.fr)

(Received March 9, 1998; revised August 3, 1998;
accepted August 18, 1998.)